Electrochemistry-Based Light-Emitting Mobile Systems

Gerardo Salinas, Ileana-alexandra Pavel, Neso Sojic, Alexander Kuhn

Electrochemistry based light-emitting mobile systems

Gerardo Salinas,[a] Ileana-Alexandra Pavel,[a] Neso Sojic,[a] Alexander Kuhn*[a]

[a]   Dr. G. Salinas, Dr. I-A. Pavel, Prof. N. Sojic, Prof. A. Kuhn

Univ. Bordeaux, CNRS, Bordeaux INP, ISM, UMR 5255, F-33607 Pessac, France.

E-mail: kuhn@enscbp.fr

Abstract: Light emitting mobile systems are presented as an important concept for direct visualization and tracking of active objects. Motion or light emission can be achieved by different electrochemical mechanisms. Various devices, that generate light by fluorescence, (electro)chemiluminescence or via light emitting diodes are shown to be an interesting alternative for the detection or release of target molecules, providing straightforward optical imaging. This review summarizes and discusses the recent advances with respect to the design and the potential applications of such original systems.

1. Introduction

The design of new dynamic devices that transform the energy from their surroundings into mechanical motion, has gained considerable attention in recent years.[1-7] Their importance derives from their interesting potential applications in sensing,[8-10] environmental remediation[9,11] and cargo delivery.[10,12] In addition, self-propelled devices can be used to mimic the behavior of microorganisms that respond to a physical or chemical stimulus.[13-15] This enables their use as models to study collective behavior such as swarming and schooling[16,17] Direct visualization and tracking of these devices, at high spatial and temporal resolution, provides a powerful tool to study complex dynamics and interactions.[18] This is related to the present trend of miniaturization of these devices, which makes it more and more complicated to monitor them by conventional methods.[19] Thus the development of visualization alternatives are becoming increasingly important. An interesting approach is the design of dynamic devices that couple mechanical motion and light emission. These kind of devices should not be confused with light-propelled micro- and nano swimmers,[20,21] for which light is used to thermally induce a surface tension gradient[22] or photoelectrochemically[23,24] and photocatalytically decompose fuels[25] to induce motion. Light emission can be achieved by different processes, such as fluorescence, (electro)chemiluminescence, or by using electronic devices like light emitting diodes. The aim of the present review is to discuss the recent advances concerning the design and potential applications of different light emitting dynamic systems. In addition, this report especially focuses on devices where either the emitted light or the motion is triggered by electrochemical processes.

2. Motion driven by electrochemistry

2.1. Self-propulsion mechanisms

In general, two main types of self-propulsion mechanisms can be distinguished: bubble propulsion and phoretic motion. In the first case, bubbles are formed on the catalytically active site, and their detachment generates motion,[26,27] whereas in the phoretic mechanism case, swimmers are propelled by a self-generated local gradient. The first design of a self-propelled particle was based on the catalytic decomposition of hydrogen peroxide on Pt.[28] Using nickel as catalyst, Ozin's group

prepared a bimetallic Au/Ni nanorod that showed rotary motion in the presence of H2O2 when the gold part was tethered to a surface.[29] Independently of this work, Au/Pt nanorods with linear motion in solution have been reported.[30] Subsequently, the underlying mechanism was elucidated. By the simultaneous oxidation and reduction of H2O2 at the Pt and Au end respectively, a flow of electric charge from the anode (Pt) to the cathode (Au) generates electroosmosis, leading to the movement of the motor in the opposite direction (Figure 1a).[31]
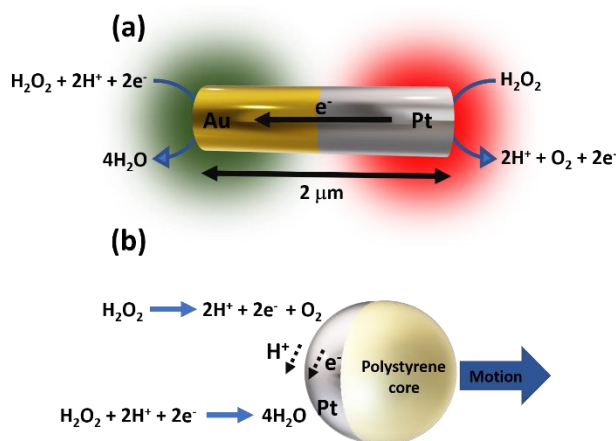

Figure 1. (a) Schematic illustration of a catalytic bimetallic Au/Pt nanorod (Adapted from reference 31) (b) Schematic illustration of the catalytic decomposition of H2O2 at the Pt surface of a platinum/polystyrene Janus particle. (Adapted from reference 32).

Recently, experiments using platinum Janus particles (platinum/insulator particles[32] or shaped platinum disks[33]) revisited the proposed propulsion mechanism of motors based on Pt-catalyzed disproportionation of H2O2. Due to spatial variations and different rates of the oxidation/reduction reactions of hydrogen peroxide on the Pt surface, the motion mechanism of these particles is considered now to be mainly self-electrophoretic (Figure 2b), even though more complex scenarios also exist. For example, anisotropic microparticles, which contain Pt and magnetic nanoparticles, prepared by Wang's group, are considered to be propelled by a combination of mechanisms of oxygen-bubble release and self-electrophoresis,[34] where both processes take place at the Pt surface. Although H2O2 based propulsion systems have been the central focus of this field of research,[26] other fuel sources have been considered, like acid[35] (H2SO4, HCl, H3PO4), hydrazine[36] and water[37] as well as different catalysts as Mg, Zn, Al or enzymes as biocatalysts.[38] Finally, as an alternative to these mechanisms, Bastos-Arrieta et al. used recently the galvanic replacement of the Cu "cap" on a Janus particle with Pt to induce an electromotive force creating motion.[39]

2.2. External electric field based propulsion

Motion of micro- and nanoparticles can also be powered by different external stimuli such as acoustic waves, light[40] and magnetic fields.[41,42] One interesting alternative to induce and control motion is also the use of an external electric field.[43] Based on the intensity of the applied electric field and the type of perturbation (AC or DC), different mechanisms of propulsion have been studied. Electrophoretic motion of dispersed electrically charged particles, dielectrophoretic forces, induced-charge electrophoresis and electroosmotic propulsion are the most common processes induced by an external electric field.

For example, Dou et al[44] used the asymmetry of a Janus Au-SiO2 particle to prove that the oscillatory motion can be rectified, and the observed self-propulsion is based on a rotation-induced

translation, following charge transfer via contact charge electrophoresis (CCEP) at the surface of parallel ITO electrodes. CCEP uses steady electric fields to induce rapid oscillatory motion of conductive particles between at least two electrodes, by repeatedly charging and actuating the particles. Lee et al.[45] have demonstrated that, under an AC electric field, spherical active colloids with metal patches of low symmetry self-propel in a helical path along the axis of the applied field. Combining different particle asymmetries with specific characteristics of the applied electric field, particle navigation through complex crosslinked matrices were presented. Zhang et al[46] demonstrated a new strategy to propel, confine and collect metallodielectric (SiO2-Ti) Janus particles in an interdigitated microelectrode (IDE) labyrinth set-up. The horizontal component of the AC electric field confines the particles in a hydrodynamic trap as it induces a lateral electroosmotic flow. In addition, the particles are propelled via induced charge electrophoresis (ICEP) when the vertical component of the AC aligns with the particles. An excess of charge is induced on the surface of the metal hemisphere (Ti), as it can be polarized with respect to the SiO2 hemisphere. Therefore, the two parts of the Janus particle attract different amounts of counter-ions in the electrical double layer. Under the influence of a low frequency electric field (tens of kHz), the charged double layer on the Ti moves faster, compared to SiO2, creating motion with the dielectric hemisphere in a forward configuration. When the frequency increases (MHz), past the charge relaxation time of the electric double layer, the Janus particles travel with the metallic hemisphere forward. This propulsion mechanism is known as self-dielectrophoresis (sDEP).[47] Taking advantage of both mechanisms, ICEP and sDEP, to control the speed and the direction of metallodielectric Janus particles, Park et al.[48] showed a selective loading, transport and cargo release. The cargo is manipulated by dielectrophoresis (DEP),[49] since DEP is a frequency-dependent mechanism. As a function of the particle polarization with respect to the solution in the presence of a non-uniform field, the particle will be repelled from (negative dielectrophoresis, nDEP) or attracted to (positive dielectrophoresis, pDEP) the regions of high field intensity. By combining AC and DC electric fields, Au-Pt nanomotors showed a controlled motion in 2D and 3D. The catalytic nanomotors are aligned by the AC field and acquire a controlled speed by the DC field. This type of set-up showed promising results in cargo manipulation (Au rod) and in powering rotary nanoelectromechanical devices.[50] Velev's group[51] showed that a complex swimmer structure, such as a "microspinnel" with gold patches on its surface, can convert electric energy into rotational motion. The propulsion mechanism strongly depends on the frequency. As the frequency increases the mechanism changes from electro-hydrodynamic (EHD) flow and reversed electro-hydrodynamic flow to induced charge electrophoresis or self-dielectrophoresis. EHD flow is caused by the presence of a dielectric particle close to the surface of the electrode, which deforms the vertical electric field. This develops tangential components of the electric field, generating locally induced charges on the electrode and triggers a symmetric electro-hydrodynamic flow. By introducing asymmetry to the particles, the vertical electric field deforms, breaking the symmetry of the system and unbalancing the EDH flows, therefore triggering propulsion.

Finally, another alternative to trigger and control motion of a conductive object is the employment of bipolar electrochemistry (BE). BE is a powerful tool for inducing asymmetric electroactivity on a conducting object. BE is based on the polarization of a conducting object in the presence of an electric field. Under sufficient polarization, different redox reactions occur at the anodic and cathodic sections of the object. Commonly, motion is achieved by the formation of gas bubbles (H2 or O2) at the surface of the conducting object. For example, a copper wire, used as a bipolar electrode (BPE), can be propelled in folded channels with different angles (from 30º to 180º) due to the asymmetric formation of hydrogen bubbles at the cathodic side.[52] For a more detailed description of this technique the reader is invited to consult other publications.[53-57]

3. Fluorescent swimmers

Fluorescent micro- and nanoswimmers are obtained by labelling the surface of the devices with fluorescent dyes[58,59] or by incorporating fluorescent components into their structure.[60,61] Commonly, fluorescence emission of micro- and nanoparticles is used to track rotation,[60,62] directional and random motion,[58] as well as an analytical tool.[63,64] Several examples of fluorescent micro- and nanoswimmers, where motion is triggered by self-thermophoresis,[58,65] enzymatic bubble propulsion[64] and magnetic fields,[59,61,66] have been described. These devices present interesting properties for externally controlled motion and remote sensing. Here we summarize the recent findings with respect to the design and potential applications of electrochemically driven fluorescent micro- and nanoswimmers.

3.1. Fluorescent micro- and nanoswimmers.

In the majority of examples of fluorescent swimmers, motion is achieved via bubble-propulsion, enabled by the catalytic[67] or photocatalytic[68] disproportionation of hydrogen peroxide or by the spontaneous reduction of water on the surface of Mg or Zn.[69-71] In addition to self-propulsion, motion control can be also obtained by embedding ferromagnetic components.[72] These swimmers are built mostly by electrochemical deposition,[73] layer-by-layer assembly[74] or emulsion templating.[75]

Specific fluorescence emission of these devices has been obtained by labelling their surface with different fluorophore molecules. For example, self-propelled avidin/Pt micro-tubes, labelled with biotinylated fluorescein, generate intense green and red fluorescence emissions.[74] Polycaprolactone/Pt/Fe3O4 micro-spheres loaded with fluorescent coumarin show intense green fluorescence light.[76] These devices can be used for the qualitative and quantitative detection of biomarkers by fluorescence quenching.[77] Recently, two different 2D germanene derivatives, 4-fluorophenylgermanane (2D-Ph-Ge) and methylgermanane (2D-Me-Ge), were used to label self-propelled graphene/Pt micro-tubes.[78] These swimmers present, under UV light irradiation, strong blue (2D-Ph-Ge) and red (2D-Me-Ge) emissions, which allow their use for bioimaging and biomedical applications, as they can be loaded with cargo for delivery. An interesting approach to produce fluorescence emission is the incorporation of fluorophores inside the swimmer structure. For example, hybrid nanostructures made of GaN/ZnO/Au have been reported as photocatalytic self-propelled light emitting swimmers.[68] Under UV irradiation these devices show a strong blue fluorescence due to the hybrid GaN/ZnO structure. Jurado-Sanchez et al. designed hybrid magnetocatalytic Janus swimmers by incorporating highly fluorescent phenylboronic acid, modified graphene quantum dots (GQDs) (Figure 2a), platinum and iron oxide particles in polycaprolactone.[79] An alternative is the use of self-propelled intrinsically fluorescent materials which does not require additional fabrication steps and labels such as organic molecules or quantum dots. Villa et al. synthesized photocatalytic bubble propelled graphene carbon nitride (GCN) microtubes guided by visible light (Figure 2b).[80] For these devices, propulsion is achieved by the photogeneration of O2 bubbles in the inner cavity of the microtubes via H2O2 decomposition. The intrinsic fluorescence of GCN originates from the delocalization of electrons in the heptazine structure of C3N4, which leads to an electron transition from the valence band (VB) to the conduction band (CB). Finally, motion of hybrid fluorescent clusters, triggered by a vertical external electric AC field (Figure 2c) have been reported.[81] Hybrid clusters of different fluorescent microspheres, build by sequential capillarity-assisted particle assembly (sCAPA), present linear and rotational motion due to the presence of asymmetric EHD (Figure 2c). Through fluorescence imaging, real time motion tracking of the hybrid clusters with different geometries was achieved, confirming

the linear dependence of the speed with the square of the electric field strength, characteristic of a EHD propulsion mechanism.[81]

3.2. Applications of fluorescent micro- and nanoswimmers.

Fluorescent micro- and nanoswimmers have gained considerable attention in optical monitoring[67] and bioimagining.[75] The photocatalytic degradation of biological and chemical agents by using Mg/TiO2/Au NPs labeled with fluorophores, has been studied.[69] Also, the physiological cargo delivery of fluorescent excipients embedded in Mg/TiO2/PLGA[70] swimmers or in compartmentalized Zn/gelatin tubes with a pH-responsive cap[71] have been reported. In addition, qualitative and quantitative analyses have gained considerable attention, since these devices take advantage of the on-off mode of the light emission and the enhanced mass transport due to their continuous motion. Escarpa's group showed the possible cargo delivery of fluorescent molecules attached to the surface of carbon micro-swimmers.[73] The decrease of the fluorescence intensity in solution (switch off) originates from the π- π stacking interactions between the fluorescent molecules and the graphene surface. Using this concept, fluorescence quenching of labeled toxins by different graphene/Pt microtubes have been reported.[72,82,83] With a similar philosophy, graphene/Pt NPs[84] and graphene/Ni/Pt NPs[85] microtubes with different fluorophores adsorbed on their surface have been used for mycotoxin analysis. With these devices, the fluorescence intensity of the solution increases as the concentration of the analyte increases, due to a constant release of the adsorbed fluorophore.

One of the first examples of molecular recognition by light emitting fluorescent microswimmers took advantage of the fast reaction between fluoresceinamine and phosphoryl halides. In this case self-propelled Si-NH2/Pt microspheres, labeled with fluoresceinamine, have been used for the analysis of sarin and soman analogs by fluorescence quenching.[86] A later study evaluated the fast and specific fluorescence quenching caused by the interaction of phenylboronic acid modified GQDs with target endotoxins.[79] Self-propelled magnetotactic modified GQDs/Pt/Fe3O4 microspheres present a strong and well-distributed blue fluorescence, which is lost in the presence of lipopolysaccharides (a major component of the outer membrane of Gram-negative bacteria) (Figure 2a).[79,87] The inherent fluorescence of covalent organic frameworks based on Py-Azine was used to design microspheres containing MnO2 and Fe3O4, allowing bubble propulsion and magnetic motion control, respectively.[88] These devices present fluorescence quenching in the presence of explosive compounds, such as 2,4,6-trinitrophenol, due to the formation of hydrogen bonds between the analyte and the Py-Azine. In a similar concept, Ppy/Ni/Pt microtubes, modified with biotinylated anti-procalcitonin antibodies, were used for the off-on fluorescence analysis of procalcitonin (PCT).[89] In these devices the switching on of the fluorescence occurs once the fluorescent antibody attaches to the PCT at the surface of the swimmer.

Fluorescence quenching of light emitting swimmers due to the presence of different heavy metal ions has also been reported. One of the first attempts was the use of highly luminescence CdTe QDs/PEDOT/Pt microtubes for the real time quantification and discrimination between Hg2+ and CH3Hg2+.[90] Once mercury ions are trapped by the anionic functional groups, the formation of CdHgTe or HgTe alloys causes fluorescence quenching. The same principle has been employed with ZnS QDs embedded in PANI/Pt nanotubes for the identification of Hg2+.[91] GCN micro-tubes also present fluorescence quenching due to the presence of heavy metal ions (Figure 2b).[80] A remarkable decrease of the fluorescence in the presence of Cu2+ was observed. This has been attributed to the reduction of Cu2+ by the photogenerated electrons from the CB, since the formal potential of the Cu2+/Cu+ redox couple lies between the CB and VB of GCN. Finally, the design of Eu-MOF/EDTA-NiAl/MnO2 microtubes for the identification and quantification of different heavy metal

ions has been reported.[92] A direct correlation of the ion charge with the decrease of fluorescence intensity has been obtained. A complete fluorescence quenching in the presence of Fe3+, due to a competing light absorption and a possible electron transfer from the CB of the MOF to the 3d orbital of Fe3+, has been observed.
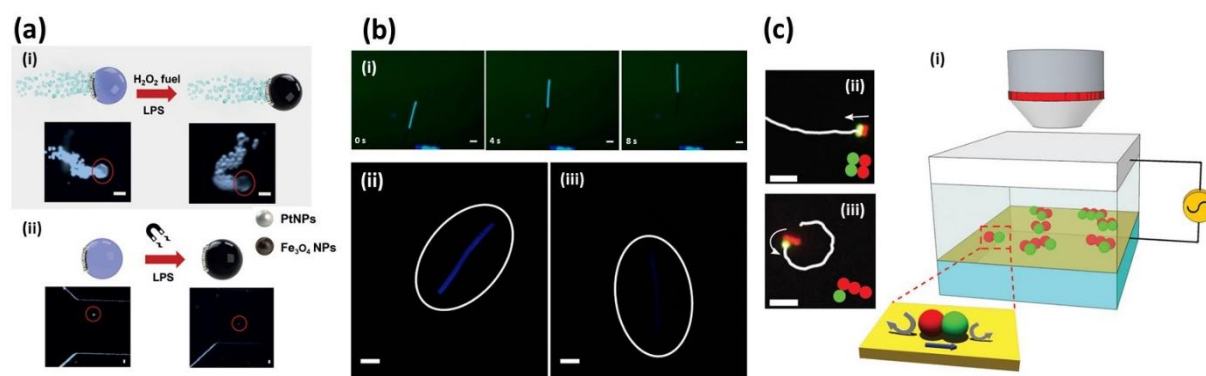

Figure 2. a) Magneto-catalytic graphene quantum dot based Janus micromotors for bacterial endotoxin detection. (i) Bubble propulsion and optical microscopy images of the Janus microswimmers before and after the addition of the lipopolysaccharide. (ii) Optical microscopy images of the magnetotactic behavior of the Janus object; scale bars 20 μm (reproduced from reference 79). b) (i) Time-lapse images of GCN micro-swimmers in 20 wt % H2O2 solution under a fluorescence optical microscope. Scale bars: 10 μm. Time-lapse images showing the fluorescence intensity of GCN micro-swimmers (ii) before and (iii) after 7 min of motion in 15 ppm of Cu2+ solution at 5 wt % H2O2 and 0.25 wt % SDS; scale bars 10 μm (reproduced from reference 80). c) (i) Scheme of the motion of hybrid fluorescent clusters in an AC electric field. The zoom schematically illustrates a possible unbalanced EHD flow around a dumbbell-like cluster. (ii–iii) Fluorescence microscopy snapshots overlaid with the trajectories of colloidal microswimmers of different geometries. The insets schematically show the details of the structures of the clusters; scale bars 5 μm (reproduced from reference 81).

4. (Electro)chemiluminescent dynamic systems

Electrochemiluminescence or electrogenerated chemi-luminescence (ECL) is a type of luminescence that occurs at the electrolyte/electrode interface. Electrochemical reactions lead in fine to the generation of the excited state of a luminophore, which emits light upon relaxation.[93-95] It differs from chemiluminescence and photoluminescence, since it is not a bulk process and does not require a light source. Commonly, ECL reactions can occur via an annihilation or coreactant mechanism[94-96] by using different kinds of luminophores, typically ruthenium, osmium and iridium complexes, organic molecules or even quantum dots and nanoparticles.[97,98] This light emitting phenomenon has been extensively used for different analytical applications, receiving considerable attention in immunoassays, DNA probe assays and biosensors.[96-98] In the past decade, (electro)chemiluminescent dynamic systems have gained considerable attention due to their possible applications in chemical and biochemical sensing. In this section we summarize the recent findings on the design and applications of different dynamic ECL and chemiluminescent systems. For a more detailed molecular description of the ECL mechanisms the reader is invited to consult more specialized publications.[94-98]

4.1. Electrochemiluminescent dynamic devices.

The very first example of ECL swimmers took advantage of the asymmetric reactions induced by BE.[99] Sentic et al. exposed a glassy carbon bead (GC) to an electric field, in the presence of Ru(bpy)$_3^{2+}$ and tri-n-propylamine (TPrA) coreactant, causing simultaneous motion and light emission (Figure 3a).[99] Water reduction and interfacial oxidation of the ECL system occur simultaneously at the cathodic and anodic poles of the bead, respectively. Thus, vertical motion is achieved due to a bubble formation at the cathodic pole, which propels the GC bead.[99] The same concept has also been used in the presence of a different luminophore system, luminol and H$_2$O$_2$.[100] In this work, vertical motion and light emission is caused by the oxidation of luminol and H$_2$O$_2$ at the anodic pole of the bead, whereas reduction of H$_2$O$_2$ occurs simultaneously at the cathodic pole. These dynamic systems can be used for chemical or biochemical sensing, where speed or light intensity can be modulated by the presence of different analytes. For example, glucose concentration was monitored by the variation of light intensity in the presence of NAD+, glucose dehydrogenase and Ru(bpy)$_3^{2+}$ (Figure 3b).[101] This dependence allows the visual tracking of vertical concentration gradients of glucose. When the swimmer reaches regions of higher glucose concentration, the ECL intensity increases.

An interesting approach is coupling the ECL emission produced by BE with another type of dynamic behavior, e.g. rotation. Although this type of motion could be simply achieved by connecting an electric conductor to an external motor,[102] wireless propulsion is an additional desirable feature. For example, a homemade four-blade rotor exposed to an electric field, in the presence of Ru(bpy)$_3^{2+}$ and TPrA,[103] was propelled by the continuous accumulation/release process of H$_2$ bubbles formed at the cathodic pole, whereas ECL emission occurs at the anodic pole. An almost linear dependence of the rotation speed as a function of applied potential was obtained. However, the rotational speed in this system is rather slow, since it takes about 120 s to complete one turn of the rotor. An alternative approach to increase the rotation speed is the use of an external magnetic field. Recently, an iron wire covered with a thin Au layer exposed to external magnetic and electric fields, in the presence of Ru(bpy)$_3^{2+}$ and TPrA, showed controlled rotation and strong ECL emission (Figure 3c).[104] In this study, motion is tracked by the light emission at the anodic pole, revealing an angular dependence due to the varying polarization of the bipolar electrode. This system presents the advantage that the ECL emission is not limited by mass transport due to the efficient convection resulting from the rotational motion.
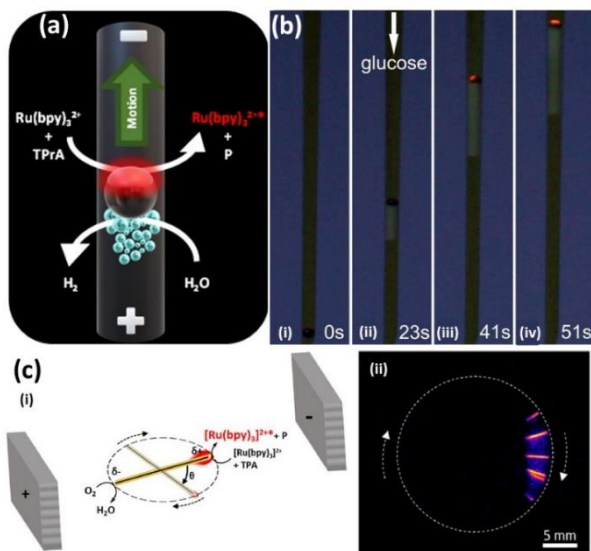
Figure 3. a) Schematic illustration of the motion and light emission principle of an electrochemiluminescent swimmer. P corresponds to a side product of the TPrA radicals formed during the ECL process. (Adapted from reference 99). b) Images illustrating the switching-on of ECL during the swimmer motion in a vertical glucose concentration gradient at different times (i-iv) (Reproduced from reference 101). c) (i) Schematic illustration of the rotation and ECL emission principle of a gold-coated iron wire. (ii) Influence of the angle on the spatial distribution of the ECL emission. (Reproduced from reference 104).

4.2. Chemiluminescent swimmers.

As stated above, ECL is an interfacial process that requires the polarization of an electrode surface, thus an external electric power supply is needed. In addition, in the other previously discussed dynamic systems, directional motion is achieved also by applying an external power source in the form of an electric or magnetic field. Therefore, the design of self-propelled chemiluminescent swimmers remains an interesting challenge. Recently, two different self-propelled chemiluminescent swimmers have been developed. In the first example, Prussian Blue-filled alginate hydrogel beads exhibit dynamic oscillatory behavior coupled with light emission.[105] For this the symmetry of the Prussian Blue beads had to be broken, transforming them into Janus particles, via a pH gradient generated by water electrolysis in an electrochemical cell. This causes different porosities at the two faces of the Janus beads, inducing an asymmetric release of oxygen bubbles, and thus triggering motion. Prussian blue catalyzes simultaneously the light emission and oxygen production in the presence of luminol and hydrogen peroxide in basic media. The second example is an autonomous chemiluminescent Janus microswimmer, using magnesium as an active ingredient. In this study, asymmetrically modified Mg microparticles present directional motion and light emission (Figure 4a).[106] The Janus microswimmers were designed by a straightforward method that involves bipolar electromilling and indirect bipolar electrodeposition of an electrophoretic paint. Motion is achieved by a bubble propulsion mechanism based on the spontaneous reduction of H_2O on the Mg surface. Light emission is triggered by a reductive-oxidation mechanism between Mg, $Ru(bpy)_3^{2+}$ and $S_2O_8^{2-}$. In this case, a direct correlation between the degree of asymmetry of these devices and the directionality of the motion has been observed (Figure 4b). This type of light emitting swimmers might be interesting for the study of collective behavior, such as swarming and schooling, in order to better understand inter-swimmer communication.
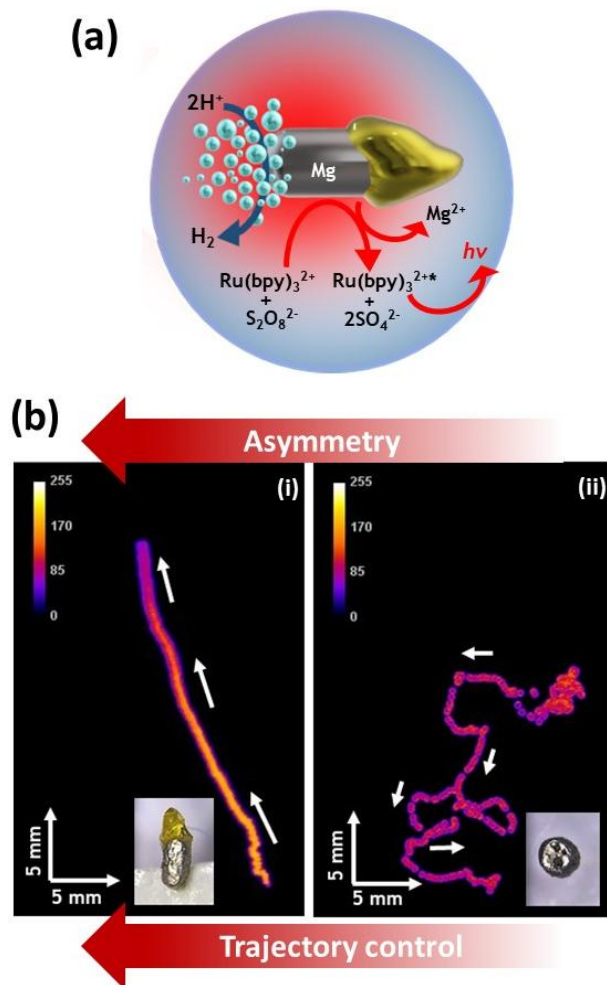
Figure 4. a) Schematic illustration of the motion and light emission principle of a self-propelled CL microswimmer. b) Tracks of the maximum light intensity of two different CL particles moving at the surface of a solution composed of 1 mM Ru(bpy)3(PF6)2, 20 mM K2S2O8 and 20 mM H2SO4 in H2O/ACN (1/1); (i) polymer modified anisotropic CL particle and (ii) unmodified isotropic particle. Global time of every experiment is 90 seconds (Reproduced from reference 106).

5. Dynamic electronic light emitting devices.

Electronic devices, such as transistors and diodes, are components that use electric current in order to process information or control systems. Commonly this kind of devices are powered by a direct electrical connection in circuit boards. An interesting approach is the use of an external electric field in order to operate these devices in a wireless manner. For example, the efficient operation of an electronic temperature sensor, powered by a wireless bipolar current, has been described.[107] In addition, the asymmetric polarization of these devices leads to motion, either by a bubble propulsion mechanism or an electroosmotic flow.[107,108] Motion of different macro-,[107] micro-,[108] and nanodiodes[109] powered by applying an external electric field has been reported. Recently, the study of self-propelled macro- and micro- light emitting diodes (LEDs) has gained considerable attention, due to the interesting feature of coupling motion with light emission. In this section we summarize the recent findings on the design of propelling macro- and micro-LEDs as dynamic electronic devices.

5.1. Light emitting diodes as dynamic electronic devices

Roche et al. exposed a commercial macro-LED in solution to an electric field, causing simultaneous formation of H2 and O2 at each branch of the device.[107] In addition to this, these reactions generate an electron flow across the diode, switching-on the electronic response. Multidirectional motion, independent from the cell geometry, was achieved by designing different geometric set-ups such as rocket-like and cubic LEDs swimmers. In a later study, Dauphin et al used a macro-LED as a magnetically-stirred bipolar electrode.[110] Rotation is caused by using an external magnetic field, based on the intrinsic ferromagnetic properties of the diode, whereas light emission is achieved by the coupled electrochemical processes triggered by the electric field. A stable light response was observed due to constant stirring of the solution. Finally, changes in the composition of the electrolyte solution (nature of redox-active species and/or ionic strength) can be correlated with the light emission intensity, which opens up a possible use for analytical applications.[110] The same concept can be used for LEDs with different switching voltages (colors) and micro-LEDs.

Micro-LEDs are an interesting alternative for the miniaturization of light emitting dynamic systems. Velev's group demonstrated the possible use of micro-LEDs as a new class of self-propelled light emitting swimmers.[108] These devices are powered by an external AC electric field imposed between two feeder electrodes. This AC field induce a DC voltage between the diode connectors, causing an electroosmotic flow. Motion towards the feeder electrodes (cathode or anode), depending on the surface charge of the diode has been observed. In addition, the rectified DC voltage between the diode powers additional device functions such as light emission. In a later study, the parameters of the applied AC field were changed in order to achieve directional control of these diodes.[111] Short DC pulses were introduced in addition to the applied AC field, inducing a redistribution of counter-ions which causes rotation of the diode. Finally, the electroosmotic flow, present at the surface of the diodes, has been used for pumping or mixing of fluids inside microfluidic channels.[112]

Recently, micro-LEDs functionalized with conducting polymers were presented as a light emitting crawlers.[113] Polypyrrole/micro-LED hybrids act as bipolar electrodes, where light emission and electromechanical motion is triggered by the applied electric field. The polypyrrole strips present two types of asymmetry components, a difference in surface roughness and an unequal oxidation state of the two extremities of the strip, causing the crawling effect. The simultaneously oxidation and reduction reactions at the opposite ends of the polypyrrole object lead to an electron flow through the integrated LED, causing the switching-on of the device.
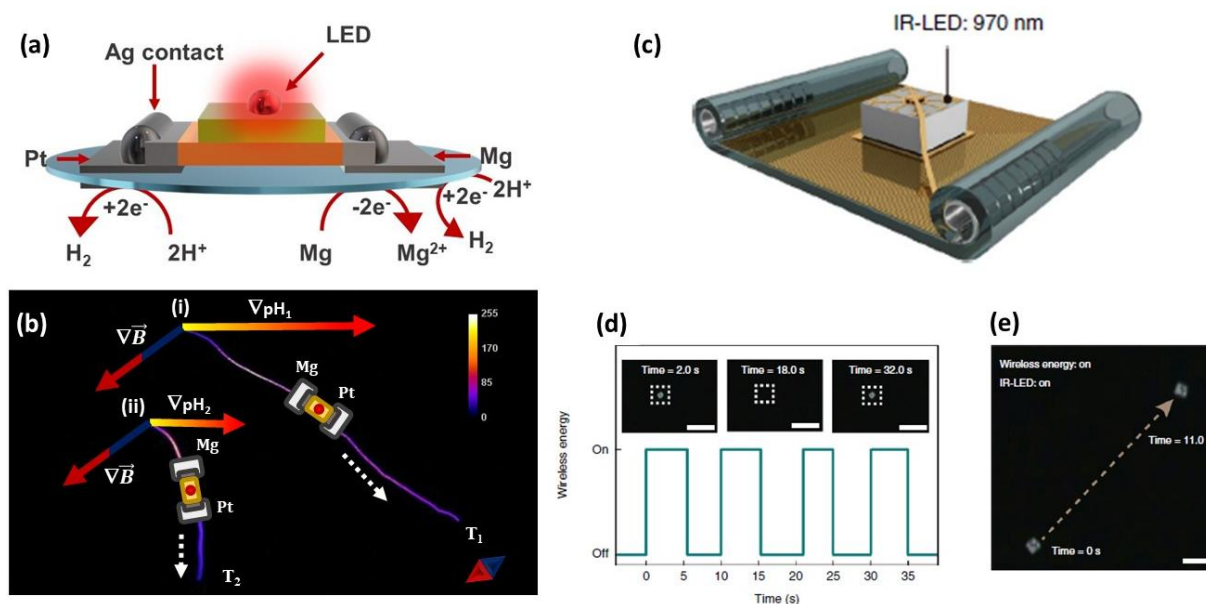
Figure 5. a) Scheme of the principle of a modified light-emitting diode actively swimming at an air/water interface, powered by the spontaneous oxidation of a Mg foil and the reduction of H3O+ on a Pt and Mg foil. b) Tracking of the maximum light intensity of two-independent chemo-electronic swimmers moving at the air/water interface in the presence of two different pH gradients and the terrestrial magnetic field. Schematic illustration of the vector addition of magnetic field and pH gradient leading to i) trajectory 1 (T1) and ii) trajectory 2 (T2). (Reproduced from reference 114). c) Schematic of the motile twin-jet-engine microsystems (MTJEMS) with an integrated IR-LED. d) Microscope images of the MTJEMS with an IR-LED, showing light-on and off functionality, and the corresponding 'on' and 'off'' states of the wireless energy supply. Scale bars, 2 mm. e) Microscope image of the MTJEMS with the integrated IR-LED. During MTJEMS motion, the IR-LED maintained the 'on' state using the on-board wireless power. Scale bar, 1 mm. (Reproduced from reference 116).

A promising alternative, which allows achieving real self-propulsion, is based on the functionalization of the diode connectors with redox couples undergoing spontaneous reactions. As an example, self-propelled light emitting swimmers powered by coupling the oxidation of Mg and the reduction of H3O+ have been reported (Figure 5a).[114] The involved redox reactions provide enough driving force to switch-on the LED and to simultaneously trigger motion by a bubble-propulsion mechanism. Furthermore, the self-propelled devices exhibit positive chemotactic behavior, propelling themselves towards a pH or ionic strength gradient, and magnetotactic behavior due to their internal ferromagnetic components.[114] The presence of both forces allows an interplay between chemotaxis and magnetotaxis, which opens up the possibility to generate and control complex trajectories (Figure 5b). Finally, novel motile twin-jet-engine microsystems (MTJEMS) have been developed as self-propelled swimmers.[115] In a hydrogen peroxide solution, the Pt inside the tubular engine catalyzes H2O2 decomposition into water and oxygen, triggering the bubble propulsion. In addition, these devices use a wireless energy transmission, where the energy is remotely transferred from the external transmitter (blocking oscillator, or Joule thief circuit) to a receiver coil within the MTJEMS. This wireless energy transmission enables powering of integrated electrical circuits such as light emitting diodes.[116] In this study a 970 nm IR-LED is connected to the on-board receiver coil of the MTJEMS (Figure 5c). The wireless transmission of electrical energy was used to power the IR-LED during the MTJEMS motion. The IR-LED can be switched on and off by

remotely switching the external power supply (Figure 5d) while the MTJEMS moves freely in an H2O2 solution (Figure 5e).[116]

6. Summary and Outlook

In this review, we discussed various concepts combining motion and light emission, mostly based on electrochemical approaches. Recent developments of such light emitting dynamic systems have demonstrated the possibility to precisely control the particles' trajectories and speed, either in simple or more complex set-ups (such as labyrinths or cross-linked matrices). All these light emitting systems present various advantages and disadvantages depending on different aspects such as the mechanism of light generation, the design of the devices and the needed equipment. For example, the fluorescent and (electro)chemiluminescent systems allow easy miniaturization of the mobile systems, whereas the electronic light emitting devices are mostly limited to the sub-millimeter scale. With respect to image acquisition, the rather strong intensity of the light, emitted by ECL and LEDs, can be readily tracked with simple commercial cameras, whereas fluorescence requires more expensive and complex optical microscopy set-ups. Last-but-not-least, light emission, triggered by spontaneous redox reactions, is a feature that provides complete autonomy to these devices, in comparison to systems that require the use of an external light or electricity source to produce light.

From nano to macro devices, the change of fluorescence, (electro)chemiluminescence or electronic light emission, often caused by the detection or release of target molecules, provides a straightforward visualization strategy for remote sensing and optical imaging. The remote control of particles, as well as cargo manipulation such as selective loading, transport and release opens the possibility to use these swimmers as chemical or biochemical sensing devices, for environmental or biomedical applications. Novel and original design strategies of light emitting swimmers enable the development of systems that may perform very challenging tasks. Finally, since the collective behavior of swimmers also requires further studies and understanding, light emitting devices could provide an easier access to information about complex processes such as swarming, schooling and the response to local gradients in the proximity of other swimmers.

Acknowledgements

Gerardo Salinas received his Master and PhD degrees in electrochemistry from the Universidad Nacional Autónoma de México (UNAM). Since 2018 he is performing postdoctoral studies at the Institute of Molecular Sciences (University of Bordeaux, Bordeaux INP, CNRS, France) under the supervision of Prof. Alexander Kuhn. His research interests include analytical electrochemistry, bipolar electrochemistry, synthesis and electrochemical characterization of conducting polymers and design of light emitting micro-swimmers.

Ileana-Alexandra Pavel is currently as a postdoctoral fellow in Prof. Kuhn's group at the Institute of Molecular Sciences (University of Bordeaux, Bordeaux INP, CNRS, France). She obtained her Master degree from the University of Bucharest and her PhD from the Université de Lorraine in Nancy (France). Her current research focuses on self-propelled chemo-luminescent swimmers.

Neso Sojic is Professor at the Institute of Molecular Sciences (University of Bordeaux, Bordeaux INP, CNRS, France). He received his Master degree in Electrochemistry at the University Pierre et Marie Curie (Paris, France). He graduated with a Ph.D. in Electrochemistry at the Ecole Normale Supérieure (Paris). After postdoctoral studies at the University of Texas at Dallas, he joined the faculty at the University of Bordeaux (France). His research interests include analytical electrochemistry, electrochemiluminescence, bioelectrochemistry, spectroelectrochemistry, and fiber optic sensors.

Alexander Kuhn is Professor at the Institut of Molecular Science (University Bordeaux, CNRS, Bordeaux INP, France), as well as Adjunct Professor at VISTEC (Thailand) and Henan University (China). After studying chemistry at the TU München, he obtained his PhD in 1994 from the University Bordeaux. Following his post-doctoral studies at Caltech (1995/1996) he obtained an Assistant Professor (1996) and later a Full Professor (2000) position in Bordeaux. He is a senior member of the Institut Universitaire de France, distinguished senior member of the French Chemical Society and fellow of the International Society of Electrochemistry. His current main research interests are modified electrodes with a special focus on applications in electroanalysis, bioelectrochemistry and electrocatalysis; nanomaterials; microswimmers; Janus particles; bipolar electrochemistry; chirality.

[1]   S. Sengupta, M. E. Ibele, A. Sen, Angew. Chem. Int. Ed. 2012, 51, 8434-8445.

[2]   W. F. Paxton, S. Sundararajan, T. E. Mallouk, A. Sen, Angew. Chem. Int. Ed. 2006, 45, 5420-5429.

[3]   S. Sanchez, L. Soler, J. Katuri, Angew. Chem. Int. Ed. 2014, 53, 2-33

[4]   T. E. Mallouk, A. Sen, Sci Am. 2009, 300, 72-77.

[5]   M. Medina-Sanchez, V. Magdanz, M. Guix, V. M. Formin, O. G. Schmidt, Adv. Funct. Mater. 2018, 28, 1707228.

[6]   K. Han, C. W. Shields IV, O. D. Velev, Adv. Funct. Mater. 2018, 28, 1705953.

[7]   J. G. S. Moo, C. C. Mayorga-Martinez, H. Wang, B. Khezri, W. Z. Teo, M. Pumera, Adv. Funct. Mater. 2017, 27, 1604759.

[8]   L. Kong, J. Guan, M. Pumera, Curr. Opin. Electrochem. 2018, 10, 174-182.

[9]   M. Zarei, M. Zarei, Small 2018, 14, 1800912.

[10]   S. Campuzano, B. Esteban-Fernandez de Avila, P. Yañez-Sedeño, J. M. Pingarron, J. Wang, Chem. Sci., 2017, 8, 6750-6763.

[11]   W. Gao, J. Wang, ACS Nano, 2014, 84, 3170-3180.

[12]   W. Duan, W. Wang, S. Das, V. Yadav, T. E. Mallouk, A. Sen, Annu. Rev. Anal. Chem. 2015, 83, 11-33.

[13]   M. You, C. Chen, L. Xu, F. Mou, J. Guan, Acc. Chem. Res. 2018, 51, 3006-3014.

[14]   M. N. Popescu, W. E. Uspal, C. Bechinger, P. Fischer, Nano Lett, 2018, 18, 5345-5349.

[15]   J. Katuri, K. D. Seo, S. Sanchez, Lab Chip, 2016, 16, 1101-1105.

[16]   W. Wang, W. Duan, S. Ahmed, T. E. Mallouk, A. Sen, Nano Today 2013, 8, 531-554.

[17]   W. Wang, W. Duan, S. Ahmed, A. Sen, T. E. Mallouk, Acc. Chem. Res. 2015, 48, 1938-1946.

[18]   S. M. Anthony, Y. Yu, Anal. Methods, 2015, 7, 7020-7028.

[19]   F. Novotny, H. Wang, M. Pumera, Chem 2020, 6, 867-884.

[20]   S. Palagi, D. P. Singh, P. Fischer, Adv. Optical Mater. 2019, 7, 1900370.

[21]   K. Villa, M. Pumera, Chem. Soc. Rev. 2019, 48, 4966-4978.

[22]   D. Okawa, S. J. Pastine, A. Zettl, J. M. J. Frechet, J. Am. Chem. Soc. 2009, 131, 5396-5398.

[23]   J. Zheng, B. Dai, J. Wang, Z. Xiong, Y. Yang, J. Liu, X. Zhan, Z. Wan, J. Tang, Nat. Commun. 2017, 8, 1438.

[24]   D. Zhou, L. Ren, Y. C. Li, P. Xu, Y. Gao, G. Zhang, W. Wang, T. E. Mallouk, L. Li, Chem. Commun. 2017, 53, 11465-11468.

[25]   M. Enachi, M. Guix, V. Postolache, V. Ciobanu, V. M. Fomin, O. G. Schmidt, I. Tiginyanu, Small 2016, 12, 5497-5505.

[26]   Q. Chi, Z. Wang, F. Tian, J. You, S. Xu, Micromachines 2018, 9, 537.

[27]   A. Nourhani, E. Karshalev, F. Soto, J. Wang, Research 2020, 2020, 7823615.

[28]   R. F. Ismagilov, A. Schwarts, N. Bowden, G. M. Witesides, Angew. Chem. Int. Ed. 2002, 41, 652-654.

[29]   S. Fournier-Bidoz, A. C. Arsenault, I. Manners, G. A. Ozin, Chem. Commun. 2005, 441-443.

[30]   W. F. Paxton, K. C. Kistler, C. C. Olmeda, A. Sen, S. K. St. Angelo, Y. Cao, T. E. Mallouk, P. E. Lammert, V. H. Crespi, J. Am. Chem. Soc. 2004, 126, 13424-13431.

[31]   Y. Wang, R. S Hernandez, D. J. Bartlett, J. M. Bingham, T. R. Kline, A. Sen, T. E. Mallouk, Langmuir 2006, 22, 10451-10456.

[32]   Y. Ibrahim, R. Golestanian, T. B. Liverpool, J. Fluid. Mech. 2017, 828, 318-352.

[33]   A. M. Brooks, M. Tasinkevych, S. Sabrina, D. Velegol, A. Sen, K. J. M. Bishop, Nat. Commun. 2019, 10, 495.

[34]   C. Zhou, P. Zhu, Y. Tian, M. Xu, L. Wang, ACS Nano 2019, 13, 6319–6329.

[35]   W. Gao, A. Uysegul, J. Wang, J. Am. Chem. Soc. 2012, 134, 897-900.

[36]   W. Gao, A. Pei, R. Dong, J. Wang, J. Am. Chem. Soc. 2014, 136, 2276-2279.

[37]   W. Gao, A. Pei, J. Wang, ACS Nano 2012, 6, 8432-8438.

[38]   M. Mathesh, J. Sun, D. A. Wilson, J. Mater. Chem. B 2020, Advance Article, DOI: 10.1039/D0TB01245A.

[39]   J. Bastos-Arrieta, C. Bauer, A. Eychmüller, J. Simmchen, J. Chem. Phys. 2019, 150, 144902.

[40]   M. Fernández-Medina, M. A. Ramos-Docampo, O. Hovorka, V. Salgueiriño, B. Städler, Adv. Funct. Mater. 2020, 30, 1908283.

[41]   X. Z. Chen, B. Jang, D. Ahmed, C. Hu, C. De Marco, M. Hoop, F. Mushtaq, B. J. Nelson, S. Pané, Adv. Mater. 2018, 30, 1705061.

[42]   Q. Yang, L. Xu, W. Zhong, Q. Yan, Y. Gao, W. Hong, Y. She, G. Yang, Adv. Intell. Syst. 2020, 2000049.

[43]   L. Bouffier, V. Ravaine, N. Sojic, A. Kuhn, Curr. Opin. Colloid Interface Sci. 2016, 21, 57-64.

[44]   Y. Dou, C. A. Cartier, W. Fei, S. Pandey, S. Razavi, I. Kretzschmar, K. J. M. Bishop, Langmuir 2016, 32, 13167-13173.

[45]   J. G. Lee, A. M. Brooks, W. A. Shelton, K. J. M. Bishop, B. Bharti, Nat. Commun. 2019, 10, 2575.

[46]   L. Zhang, Z. Xiao, X. Chen, J. Chen, W. Wang, ACS Nano 2019, 13, 8842-8853.

[47]   A. Boymelgreen, G. Yossifon, T. Miloh, Langmuir, 2016, 32, 9540-9547.

[48]   S. Park, G. Yossifon, ACS Sens. 2020, 5, 936-942.

[49]   A. M. Boymelgreen, T. Balli, T. Miloh, G. Yossifon, Nat. Commun. 2018, 9, 760.

[50]   J. Guo, J. J. Gallegos, A. R. Tom, D. Fan, ACS Nano 2018, 12, 1179-1187.

[51]   C. W. Shields, K. Han, F. Ma, T. Miloh, G. Yossifon, O. D. Velev, Adv. Funct. Mater. 2018, 35, 1803465.

[52]   J. Z. Jiang, M. H. Guo, F. Z. Yao, J. Li, J. J. Sun, RSC Adv. 2017, 7, 6297-6302.

[53]   G. Loget, D. Zigah, L. Bouffier, N. Sojic, A. Kuhn, Acc. Chem. Res. 2013, 46, 2513-2523.

[54]   S. E. Fosdick, K. N. Knust, K. Scida, R. M. Crooks, Angew. Chem. Int. Ed. 2013, 52, 10438-10456.

[55]   L. Koefoed, S. U. Pedersen, K. Daasbjerg, Curr. Opin. Electrochem. 2017, 2, 13-17.

[56]   N. Shida, Y. Zhou, S. Inagi, Acc. Chem. Res. 2019, 52, 2598-2608.

[57]   N. Karimian, P. Hashemi, A. Afkhami, H. Bagheri, Curr. Opin. Electrochem. 2019, 17, 30-37.

[58]   M. Xuan, Z. Wu, J. Shao, L. Dai, T. Si, Q. He, J. Am. Chem. Soc. 2016, 138, 6492-6497.

[59]   A. Servant, F. Qiu, M. Mazza, K. Kostarelos, B. J. Nelson, Adv. Mater. 2015, 27, 2981-2988.

[60]   C. J. Behrend, J. N. Anker, R. Kopelman, Appl. Phys. Lett. 2004, 84, 154-156.

[61]   X. Yan, Q. Zhou, M. Vincent, Y. Deng, J. Yu, J. Xu, T. Xu, T. Tang, L. Bian, Y.-X. J. Wang, K. Kostarelos, L. Zhang, Sci. Robot. 2017, 2, eaaq1155.

[62]   S. M. Anthony, Y. Yu, Anal. Methods 2015, 7, 7020-7028.

[63]   V. de la Asunción-Nadal, M. Pacheco, B. Jurado-Sánchez, A. Escarpa, Anal. Chem. 2020, 92, 9188-9193.

[64]   T. Patino, A. Porchetta, A. Jannasch, A. Lladó, T. Stumpp, E. Schäffer, F. Ricci, S. Sánchez, Nano Lett. 2019, 19, 3440-3447.

[65]   W. Liu, W. Wang, X. Dong, Y. Sun, ACS Appl. Mater. Interfaces 2020, 12, 12618-12628.

[66]   Y. Zhang, L. Zhang, L. Yang, C. I. Vong, K. F. Chan, W. K. K. Wu, T. N. Y. Kwong, N. W. S. Lo, M. Ip, S. H. Wong, J. J. Y. Sung, P. W. Y. Chiu, L. Zhang, Sci. Adv. 2019, 5, eaau9650.

[67]   S. J. Ebbens, J. R. Howse, Langmuir 2011, 27, 12293-12296.

[68]   N. Wolff, V. Ciobanu, M. Enachi, M. Kamp, T. Braniste, V. Duppel, S. Shree, S. Raevschi, M. Medina-Sánchez, R. Adelung, O. G. Schmidt, L. Kienle, I. Tiginyanu, Small 2019, 16, 1905141.

[69]   J. Li, V. V. Singh, S. Sattayasamitsathit, J. Orozco, K. Kaufmann, R. Dong, W. Gao, B. Jurado-Sanchez, Y. Fedorak, J. Wang, ACS Nano 2014, 8, 11118-11125.

[70]   E. Karshalev, B. Esteban-Fernández de Ávila, M. Beltrán-Gastélum, P. Angsantikul, S. Tang, R. Mundaca-Uribe, F. Zhang, J. Zhao, L. Zhang, J. Wang, ACS Nano 2018, 12, 8397-8405.

[71]   B. Esteban-Fernández de Ávila, M. A. Lopez-Ramirez, R. Mundaca-Uribe, X. Wei, D. E. Ramírez-Herrera, E. Karshalev, B. Nguyen, R. H. Fang, L. Zhang, J. Wang, Adv. Mater. 2020, 2000091

[72]   D. F. Baez, G. Ramos, A. Corvalan, M. L. Cordero, S. Bollo, M. Kogan, Sensor. Actuat. B Chem. 2020, 310, 127843.

[73]   R. Maria-Hormigos, B. Jurado-Sanchez, A. Escarpa, Nanoscale 2017, 9, 6286-6290.

[74]   Y. Nakai, N. Sugai, H. Kusano, Y. Morita, T. Komatsu, ACS Appl. Nano Mater. 2019, 2, 4891-4899.

[75]   J. Jiao, D. Xu, Y. Liu, W. Zhao, J. Zhang, T. Zheng, H. Feng, X. Ma, Micromachines 2018, 9, 83.

[76]   W. Gao, M. Liu, L. Liu, H. Zhang, B. Dong, C.Y. Li, Nanoscale, 2015, 7, 13918-13923.

[77]   V. V. Singh, K. Kaufmann, B. Esteban-Fernández de Ávila, E. Karshalev, J. Wang, Adv. Funct. Mater. 2016, 26, 6270-6278.

[78]   T. Maric, S. M. Beladi-Mousavi, B. Khezri, J. Sturala, M. Z. Mohamad Nasir, R. D. Webster, Z. Sofer, M. Pumera, Small 2019, 1902365.

[79]   B. Jurado-Sanchez, M. Pacheco, J. Rojo, A. Escarpa, Angew. Chem. Int. Ed. 2017, 56, 6957-6961.

[80]   K. Villa, C. L. Manzanares-Palenzuela, Z. Sofer, S. Matějková, M. Pumera, ACS Nano 2018, 12, 12482-12491.

[81]   S. Ni, E. Marini, I. Buttinoni, H. Wolf, L. Isa, Soft Matter 2017, 13, 4252-4259.

[82]   B. Esteban-Fernández de Ávila, M. A. Lopez-Ramirez, D. F. Báez, A. Jodra, V. V. Singh, K. Kaufmann, J. Wang, ACS Sens. 2016, 1, 217-221.

[83]   R. Maria-Hormigos, B. Jurado-Sanchez, A. Escarpa, Chem. Commun. 2019, 55, 6795-6798.

[84]   Á. Molinero-Fernández, M. Moreno-Guzmán, M. A. López, A. Escarpa, Anal. Chem. 2017, 89, 10850-10857.

[85]   Á. Molinero-Fernández, A. Jodra, M. Moreno-Guzmán, M. A. López, A. Escarpa, Chem., Eur. J. 2018, 24, 7172-7176.

[86]   V. V. Singh, K. Kaufmann, J. Orozco, J. Li, M. Galarnyk, G. Arya, J. Wang, Chem. Commun. 2015, 51, 11190-11193.

[87]   M. Pacheco, B. Jurado-Sánchez, A. Escarpa, Anal. Chem. 2018, 90, 2912-2917.

[88]   K. Wang, W. Wang, S. Pan, Y. Fu, B. Dong, H. Wang, Appl. Mater. Today 2020, 19, 100550.

[89]   A. Molinero-Fernández, M. Moreno-Guzmán, L. Arruz, M. A. López, A. Escarpa, ACS Sens. 2020, 5, 1336-1344.

[90]   B. Jurado-Sanchez, A. Escarpa, J. Wang, Chem. Commun 2015, 51, 14088-14091.

[91]   B. Jurado-Sanchez, J. Wang, A. Escarpa, ACS Appl. Mater. Interfaces 2016, 8, 19618-19625.

[92]   W. Yang, J. Li, Z. Xu, J. Yang, Y. Liu and L. Liu, J. Mater. Chem. C 2019, 7, 10297-10308.

[93]   A. J. Bard, Electrogenerated Chemiluminescence, Marcel Dekker, 2004.

[94]   H. Qi, C. Zhang, Anal. Chem. 2020, 92, 524-534.

[95]   R. A. Husain, S. R. Barman, S. Chatterjee, I. Khan Z-H Lin, J. Mater. Chem. B 2020, 8, 3192-3212.

[96]   L. Hu, G. Xu, Chem. Soc. Rev. 2010, 39, 3275-3304.

[97]   M. Hesari, Z. Ding, J. Electrochem. Soc. 2016, 163, H3116-H3131

[98]   Z. Liu, W. Qi, G. Xu, Chem. Soc. Rev. 2015, 44, 3117-3142.

[99]   M. Sentic, G. Loget, D. Manojlovic, A. Kuhn, N. Sojic, Angew. Chem. Int. Ed. 2012, 51, 11284-11288.

[100]   L. Bouffier, D. Zigah, C. Adam, M. Sentic, Z. Fattah, D. Manojlovic, A. Kuhn, N. Sojic, ChemElectroChem 2014, 1, 95-98.

[101]   M. Sentic, S. Arbault, B. Goudeau, D. Manojlovic, A. Kuhn, L. Bouffier, N. Sojic, Chem. Commun. 2014, 50, 10202-10205.

[102]   V. Eßmann, J. Clausmeyer, W. Schuhmann, Electrochem. Commun. 2017, 75, 82-85.

[103]   V. Eßmann, S. Voci, G. Loget, N. Sojic, W. Schuhmann, A. Kuhn, J. Phys. Chem. Lett. 2017, 8, 4930-934.

[104]   A. L. Dauphin, A. Akchech, S. Voci, A. Kuhn, G. Xu, L. Bouffier, N. Sojic, J. Phys. Chem. Lett. 2019, 10, 5318-5318.

[105]   R. María-Hormigos, A. Escarpa, B. Goudeau, V. Ravaine, A. Perro, A. Kuhn, Adv. Mater. Interfaces 2020, 7, 1902094.

[106]   G. Salinas, A. L. Dauphin, S. Voci, L. Bouffier, N. Sojic, A. Kuhn, Chem. Sci. 2020, 11, 7438-7443.

[107]   J. Roche, S. Carra, J. Sanchez, J. Lannelongue, G. Loget, L. Bouffier, P. Fischer, A. Kuhn, Sci. Rep. 2015, 4, 6705.

[108]   S. T. Chang, V. N. Paunov, D. N. Petsev, O. D. Velev, Nature Mater. 2007, 6, 235-240.

[109]   P. Calvo-Marzal, S. Sattayasamitsathit, S. Balasubramanian, J. R. Windmiller, C. Dao, J. Wang, Chem. Commun. 2010, 46, 1623-1624.

[110]   A. L. Dauphin, S. Arbault, A. Kuhn, N. Sojic, L. Bouffier, ChemPhysChem 2020, 21, 600-604.

[111]   R. Sharma, O. D. Velev, Adv. Funct. Mater. 2015, 25, 5512-5519.

[112]   S. T. Chang, E. Beaumont, D. N. Petsev, O. D. Velev, Lab on a Chip 2008, 8, 117-124.

[113]   B. Gupta, M. C. Alfonso, L. Zhang, C. Ayela, P. Garrigue, B. Goudeau, A. Kuhn, ChemPhysChem 2019, 20, 941-945.

[114]   G. Salinas, A. L. Dauphin, C. Colin, E. Villani, S. Arbault, L. Bouffier, A. Kuhn, Angew. Chem. Int. Ed. 2020, 59, 7508-7513.

[115]   C. Xu, W. Gao, Nat. Electron. 2020, 3, 139-140.

[116]   V. K. Bandari, Y. Nan, D. Karnaushenko, Y. Hong, B. Sun, F. Striggow, D. D. Karnaushenko, C. Beker, M. Faghih, M. Medina-Sanchez, F. Zhu, O. G. Schmidt, Nat. Electron. 2020, 3, 172-180.

Entry for the Table of Contents

Light-emitting mobile systems, based on electrochemical approaches, offer interesting visualization strategies for potential applications ranging from remote sensing and optical imaging to controlled cargo manipulation and studies of complex collective behaviour such as swarming and schooling.

Institute and/or researcher Twitter usernames: ((optional))